Self-assembly and photoconductivity of binary porphyrin nanostructures of *meso*-tetrakis(4-sulfonatophenyl)porphine and Co(III) *meso*-tetra(4-pyridyl)porphine chloride.

Ekaterina A. Koposova[a,b], Yury E. Ermolenko[b], Andreas Offenhäusser[a], Yulia G. Mourzina[a]*

[a] *Institute of Complex Systems-8 (Bioelectronics), Research Centre Jülich, 52428 Jülich Germany and Jülich-Aachen Research Alliance (JARA)-Fundamentals of Future Information Technology*

[b] *Institute of Chemistry, Saint-Petersburg State University, Universitetskaya nab. 7/9, 199034 Saint-Petersburg, Russia*

Abstract. The tunable characteristics of the porphyrin molecular tectons have given rise to interest in investigating the self-assembled porphyrin nanoarchitectures for designing new materials. Nanostructures created by the self-assembly of *meso*-tetrakis(4-sulfonatophenyl)porphine and Co(III) *meso*-tetra(4-pyridyl)porphine chloride and their photoconductivity are reported here. These nanostructures were characterized by electron microscopy. The ratio of porphyrin tectons in the binary porphyrin nanostructures is about 3:2. The nanostructures demonstrate a high photoconductivity of about 5×10^{-5} S m^{-1}. The dependence of the photoconductivity of the porphyrin nanostructures on the path length and temperature is demonstrated.

Keywords: porphyrin nanostructures, photoconductivity, self-assembly, Co(III) porphyrin, temperature dependence

1. Introduction.

The porphyrins are an important class of synthetic and natural building blocks used in the design of new materials, because the great variability of the electronic and steric characteristics of these molecular tectons makes it possible to drive the assembly process in order to achieve various functionalities of their self-assembled nanostructures. Their ability to absorb certain wavelengths in the visible spectrum promotes photoinduced energy and electron transfer processes. Due to their similarities to chlorophyll and hemoproteins, porphyrins have been used as models for photosynthetic and enzymatic systems in studies of photo-induced energy transfer, charge separations and electron transfer processes in biology and chemistry [1, 2]. Many physicochemical properties of porphyrins and porphyrin-related macrocycles, such as

spectroscopic, electrochemical, and electronic properties are related to their aggregation states [3-7]. Water-soluble porphyrins are well-suited for studying the properties of self-assembled nanostructures because the self-assembly can be conveniently controlled by changing the properties of the medium such as the pH [6-8]. Formation of a stable assembly can be explained by the contribution of electrostatic interactions, van der Waals forces, hydrogen bonds, axial coordination, and π-π interactions [9-16]. Shellnutt´s group progressed in the understanding of the morphology of self-assembled porphyrin nanostructures using different methods for studying the properties of porphyrins and metalloporphyrins [6, 17, 18].

Porphyrin nanostructures, polymers, and arrays demonstrate some degree of conductivity and their conductivities have been investigated [19-28]. Ability of porphyrin molecules to absorb certain wavelengths in the visible wavelength spectrum promotes intermolecular transfer or delocalization of the excitation energy in their nanostructures, which generates photoconductivity [6, 7, 25, 29]. However, the data on the electronic properties of the self-assembled porphyrin nanostructures are rather sparse and the mechanisms of the charge transfer in these systems have not yet been fully elucidated. Most attention has been paid to the studies of the tubular molecular J-aggregates self-assembled from one kind of molecule, metal-free *meso*-tetrakis-(4-sulphonatophenyl)porphin [23-25, 28, 30]. The nanorods of a metal-free *meso*-tetrakis-(4-sulphonatophenyl)porphin were insulating in dark and a model was proposed by Schwab et al. [25] where the conduction occured through the tightly coupled LUMOs of the close-packed porphyrin molecules after photoexitation at a J-band wavelength of 488 nm. Transport through the LUMOs competed with the relaxation from LUMO back to HOMO. Recently, Mazur and co-workers [26, 27] described crystals of a binary porphyrin ionic assembly synthesized from the water-soluble metal-free *meso*-tetra(4-sulfonatophenyl)porphyrin and meso-tetra(N-methyl-4-pyridyl)porphyrin or *meso*-tetra(4-pyridyl)porphyrin ionic tectons. The authors proposed that the nanorods exhibited two types of photoconductivity: band conduction and hopping conductivity via the formation of photo-induced (metastable) defects. Zhai et al. [31] found that the nanodots of the porphyrin layers of 5,10,15,20-tetraphenyl-21H,23H-porphyrin cobalt(II) had a more conductive, molecular wire-like profile, while the nanodots of a free-base 5,10,15,20-tetraphenyl-21H,23H-porphyrin exhibited semi-conductive profiles when measured in the vertical direction using a conductive probe AFM. The magnitudes of the measured currents and and voltages were distinct depending on whether the nanodots contained a metal ion. Shelnutt et al. [6] observed photoconductivity of the metalloporphyrin binary nanostructures of $ZnTPPS^{4-}$ - $SnT(N\text{-}EtOH\text{-}4\text{-}Py)P^{4+}$ and explained it applying the charge-transfer exciton theory. They defined individual porphyrin

tectons as an electron donor and acceptor based on the data on the redox potentials of SnOEP and ZnOEP complexes, respectively, and applying the classical model of the charge-transfer complex as a combination of electron donor compounds and electron acceptor compounds arranged in segregated stacks. A change of the central metal atom and periphery of individual metalloporphyrins showed different possibilities for appearance of the photoconductivity due to the variation of the structure and donor-acceptor properties. The model is similar to the model explaining the conductivity of the donor-acceptor charge-transfer complex TTF-TCNQ [32], where electrons and electron holes are separated and concentrated in the stacks and can traverse along the TCNQ and TTF columns, respectively, when an electric potential is applied to the ends of a crystal in the stack direction. It was shown [33] that ion-paired species formed between water-soluble cationic and anionic porphyrins undergo very fast and efficient photo-induced charge separation, with the cationic porphyrin being reduced and the anionic one oxidize, which may support an electron-donor-acceptor charge-transfer complex mechanism for the photoconductivity of the porphyrin nanostructures.

Investigations of the electronic properties of porphyrin tectonic matter can help in understanding and utilizing the electronic transport in these nanoscale materials for the development of biomimicking nanoarchitectonics in the fields of photo(electro)catalysis [34-38], sensors [39, 40], and organic photoconducting materials [41-43]. In this regard, we report on the self-assembly, morphological, spectral, and photoconductivity properties of binary nanostructures in the system of water-soluble porphyrins: *meso*-tetrakis(4-sulfonatophenyl)porphine and Co(III) *meso*-tetra(4-pyridyl)porphine chloride.

2. Materials and Methods

2.1. Materials. Hydrochloric acid, potassium nitrate, acetone, isopropanol, and ethanol were purchased from Sigma-Aldrich. *Meso*-tetra(4-sulfonatophenyl)porphine dihydrochloride (H_4TPPS^{2-}) and Co(III) *meso*-tetra(4-pyridyl)porphine chloride, Figure 1, were purchased from Frontier Scientific and used as received. All solutions for syntheses were prepared using deionized water and adjusted to the desired pH with HCl and NaOH.

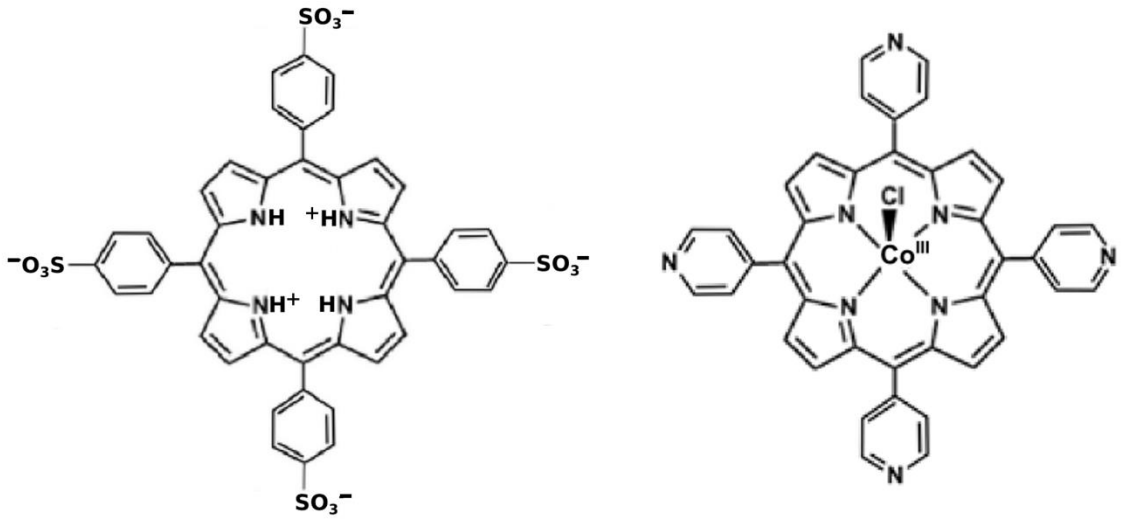

Figure 1. Schematic structure of H_4TPPS^{2-} and CoT(4-Py)P.

2.2. Characterization methods. Scanning electron microscopy (SEM) was performed on a Gemini 1550 VP, Carl Zeiss, Jena, Germany. Samples for SEM were prepared by pipetting 50 μL of the precipitate onto a Si-substrate. The samples were allowed to dry for 12 hours, washed with 0.01 M HCl, then water and allowed to dry. EDX analysis was perfomed on JEOL 840 A. Transmission electron microscopy (TEM) was performed on a FEI Tecnai G2 F20 microscope operated at 200 kV. The UV/vis spectra of individual porphyrin solutions and solutions with nanotubes were recorded with a PerkinElmer Lambda 900 spectrometer using a quartz cuvette with a path length of 1 cm. Nanostructure precipitates for the elemental analysis by NMR were obtained by centrifugation of the reaction mixture and drying the precipitates. The ratio of S:N atoms was determined by NMR. The relative standard error was (2.5%).

2.3. Conductivity measurements. For conductance measurements, thin film Au electrodes were used (50 nm thick Au film on a 10 nm Ti adhesion layer) with distances of 400 nm (electrode gap) between the contact electrodes, Figure S4. Interdigitated electrode arrays with distances of 2 μm between the electrodes were used to measure the photoconductance dependence on the path length. The electrodes were fabricated by an electron beam lithography on a Si-substrate with a 1 μm silicon oxide layer (Si 525 μm /SiO_2 1 μm /Ti adhesion layer 10 nm /Au 50 nm). Before pipetting the nanostructure solution, the electrodes were cleaned in acetone, isopropanol, followed by treatment with oxygen plasma in the «Plasma system FEMTO», at 100W, 0.8mbar. After that, ethanol and distilled water were used fot the final washing stage. A solution of porphyrin nanostructures (2 μL) was dropped onto the electrodes, the samples were left in the dark for 2 hours, rinsed with 0.01 M HCl, then distilled water and dried for 24 h at room temperature. The conductance was measured using a Keithley 4200 SCS

semiconductor analyzer system at an applied potential of 0.5 V in a two-probe current measurement configuration. The thin-film gold electrodes were electrically contacted through the bond pads using tungsten needles. The light source was a 150W xenon arc lamp with a 390-630 nm visible light filter and AM1.5 filter (Oriel Instruments, Model No. 6255). The light intensity of the beam focused on the sample was 25 mW cm^{-2} as measured by a photodetector (CAS140CT-154 Kompakt-Array-Spektrometer model UV-vis-NIR, Instrument Systems).

3. Results and Discussion

3.1. Characterization of the nanotubes morphology.

The porphyrin nanostructures were formed by mixing aqueous solutions of *meso*-tetrakis(4-sulfonatophenyl)porphine, $H_2TPPS^{4-}/H_4TPPS^{2-}$, and Co(III) *meso*-tetra(4-pyridyl)porphine chloride, CoT(4-Py)P, Fig. 1. A mixture of equal volumes of H_4TPPS^{2-} (5.25 μM in 0.02 HCl) and CoT(4-Py)P (1.75 μM in water) was adjusted to pH 2. Although the green-brown colloidal forms were observed immediately after mixing, the reaction mixture was left undisturbed in the dark at room temperature for 5 days to complete the reaction of nanostructures formation. Scanning electron microscopy (SEM) and transmission electron microscopy (TEM), Fig. 2, 3 and Fig. S1, S2 demonstrate that the nanostructures are hollow tubes with the open ends displaying a length of 0.2 to 1 μm, an outer diameter of 30 to 80 nm, and an inner diameter of about 17 to 35 nm. TEM investigation revealed the co-existence of less-structured material layers along with the well-formed nanotubes.

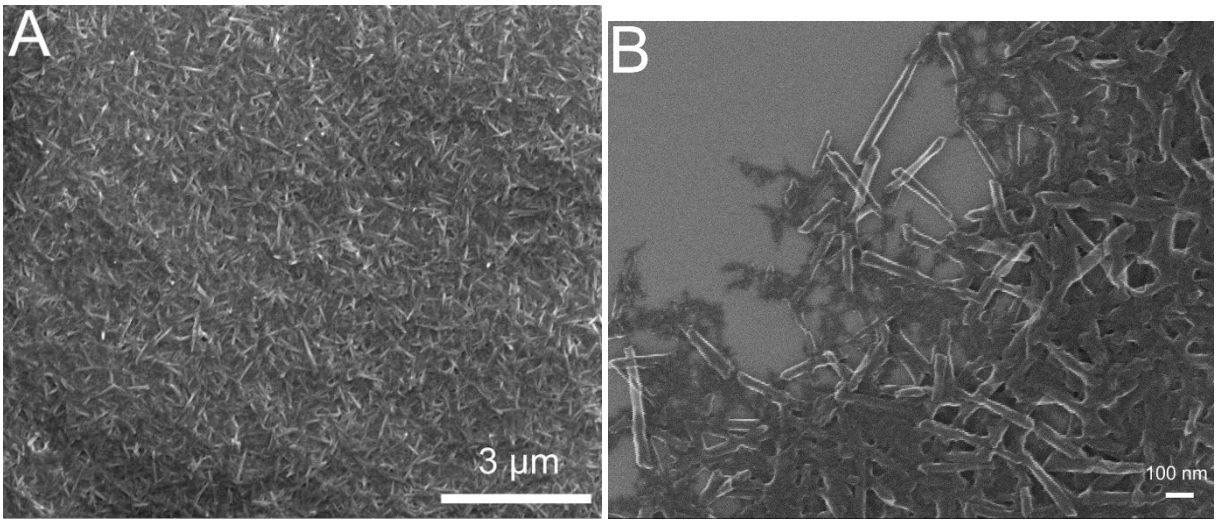

Figure 2. SEM images of the H_4TPPS^{2-} - CoT(4-Py)P^{4+} nanotubes.

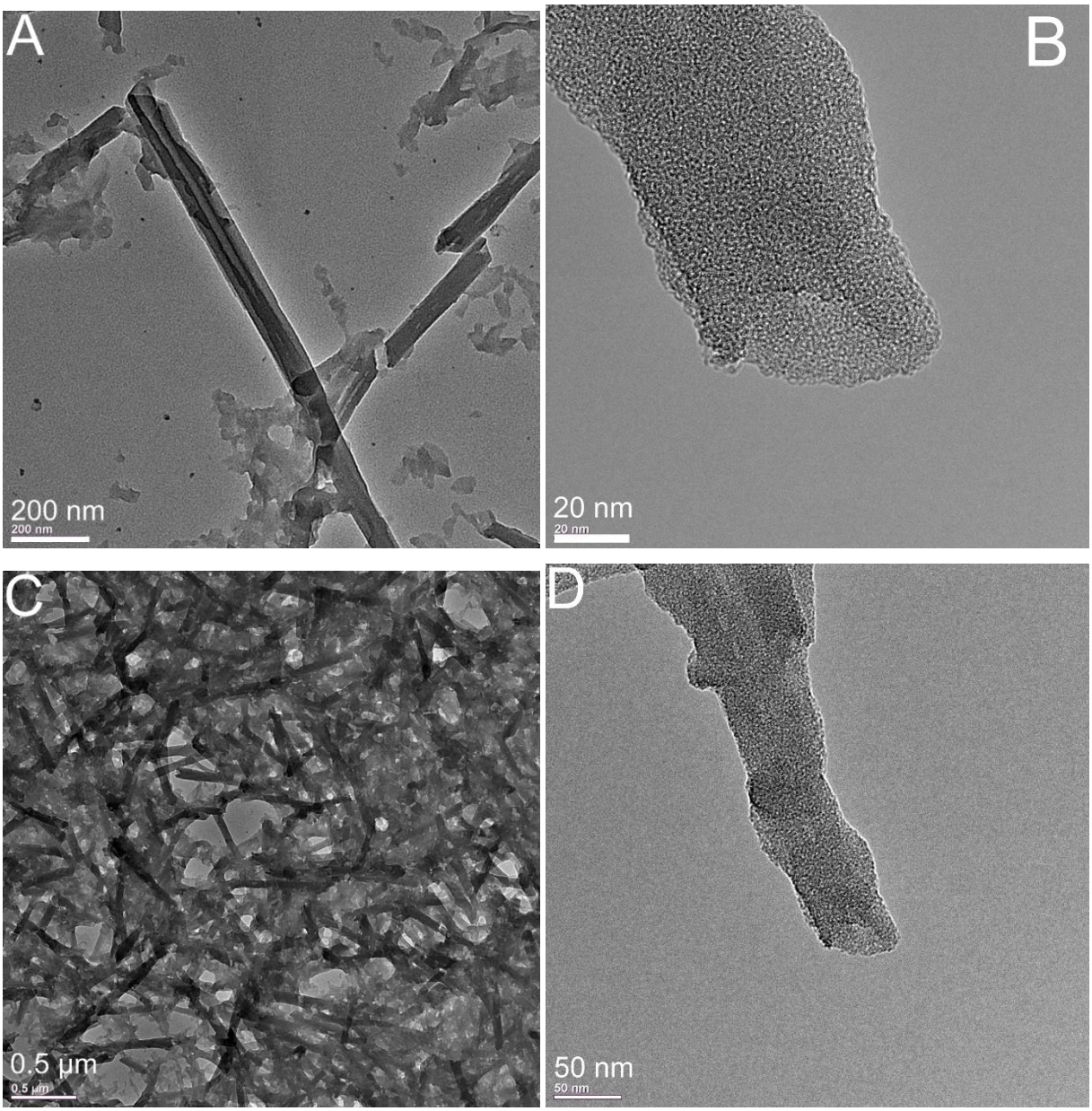

Figure 3. TEM images of the H_4TPPS^{2-} - $CoT(4\text{-}Py)P^{4+}$ nanotubes.

For comparison, much narrower nanotubes created by the self-assembly of H_4TPPS^{2-} with an outer diameter of about 15 nm are shown in Fig. S3 and are characterized by a sharp red-shifted band at 490 nm and its characteristic small bandwidth typical of the J-aggregates together with a band at 706 nm in a Q-region with respect to the transition energy of monomers, Fig. 4A. This type of interaction is characteristic of the H_4TPPS^{2-} molecules self-assembling into the slipped face-to-face columnar arrangements, which form very thin nanotubes. Formation of J-aggregates in the H_4TPPS^{2-} - $CoT(4\text{-}Py)P^{4+}$ system is confirmed by the absorption spectrum with characteristic bands at $\lambda = 494$ nm and $\lambda = 709$ nm, Fig. 4A. The J-band of H_4TPPS^{2-} - $CoT(4\text{-}Py)P^{4+}$ is broadened and slightly red-shifted in comparison to the

spectrum of H_4TPPS^{2-} aggregates. Additionally, increase of the absorption of the H_4TPPS^{2-} - $CoT(4\text{-}Py)P^{4+}$ nanostructures in a Q-band region of $CoT(4\text{-}Py)P^{4+}$ monomer at 552 nm is observed in comparison with the absorption of the nanotubes created by the self-assembly of H_4TPPS^{2-}. In contrast to the thin H_4TPPS^{2-} nanotubes, the H_4TPPS^{2-} - $CoT(4\text{-}Py)P^{4+}$ nanostructures form more continuous surfaces, when deposited on the substrates, for the study of the photoconductivity, as it is described in section 3.2.

EDX analysis confirmed a presence of both porphyrin tectons (sulfur and cobalt) in the nanostructures. In our study, analysis of the ratio of the porphyrins in the nanostructures by the Job plot [44], Fig. 4B, indicates a H_4TPPS^{2-} : $CoT(4\text{-}Py)P^{4+}$ molar ratio of 3:2 to 2:1 (a smooth molar fraction region about 0.6). A ratio of about 2:1 was confirmed by the NMR analysis as well. This ratio is a result of the neutralization of a net positive charge on the protonated $CoT(4\text{-}Py)P^{4+}$ (protonated pyridyl groups) and cationic centers of H_4TPPS^{2-} by the anionic groups of H_4TPPS^{2-}. The formation of close molecular packing of porphyrin molecules and molecular aggregates may occur by the synergistic combination of different intermolecular interactions including ion organization by electrostatic interactions (6-20 kJ mol^{-1}), π-π interaction (40 kJ mol^{-1}) arranging aromatic rings in three face-to-face arrangements, hydrogen bonding (4-40 kJ mol^{-1}), and weaker van der Waals interactions (0.4-4 kJ mol^{-1}), and may therefore lead to various 1D- to 3D-geometries [9, 45, 46]. Shelnutt's group [17] reported that the formation of porphyrin nanotubes in the system of H_4TPPS^{2-} : $Sn(IV)TPyP^{4+}$ (~2.4:1 mol/mol) was critically dependent on the pH, as the charge balance of the ionic tectons depends on their protonation state. Acidic environment (pH=2.0) provided [47, 48] the required protonated pyridyl groups of $SnTPyP^{4+}$ (pKa=5.2 for pyridine), partially dissociated sulfonato-groups (pK_a=2.6 for benzenesulfonic acid), and protonated centers of H_4TPPS^{2-} below pH 4 (pK_a 4.9) for the formation of nanostructures. It is interesting to note that replacing a cationic center of H_4TPPS^{2-} with a metal, e.g., Co(III), collapses the nanotubes into the network-like nanostructures of Sn(IV)TPPS-Co(III)TPyP [7], where opposite charges on peripheral groups were involved. The atomic ratio Sn:Co in Sn(IV)TPPS-Co(III)TPyP nanostructures was 1:1.15 and 1:3 for the samples prepared at pH 2.7 and pH 4.8, respectively [7]. As these ratios are the result of the neutralization of porphyrin cations and anions, pH is a key factor influencing the electrostatic interaction of the tectonic couples. Therefore, in the system under study a larger number of H_4TPPS^{2-} tectons presents to neutralize positive charges.

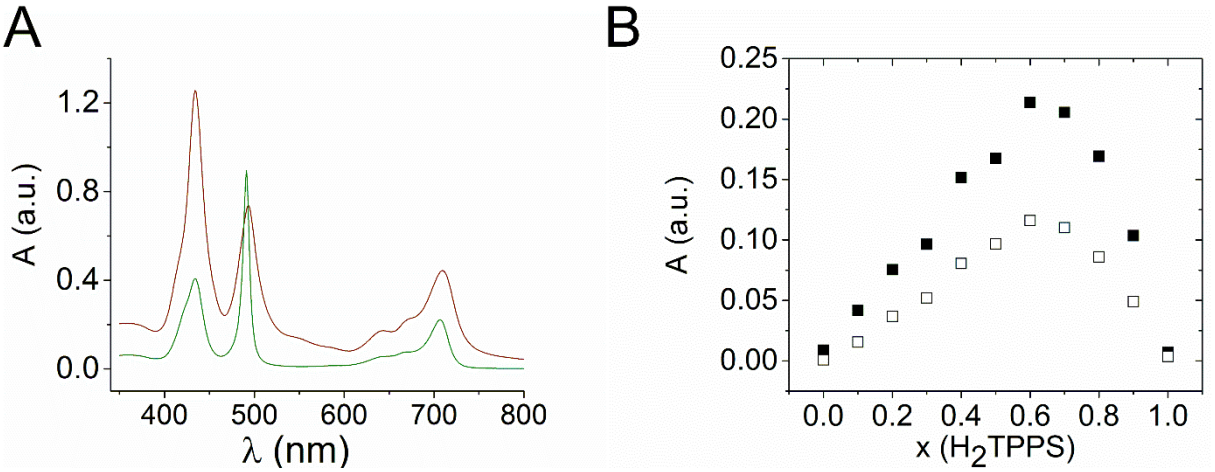

Figure 4. (A) The absorption spectra of H_4TPPS^{2-} with the J-aggregates prepared from H_4TPPS^{2-} at pH 0.7 after 5 days (green), and nanostructures of H_4TPPS^{2-} - Co(III)T(4-Py)P^{4+}, prepared at pH 2 after 5 days (brown). The samples were acidified with HCl. (B) Job plots for 493 nm (full square) and 709 nm (open square) in Klark-Labs buffer, pH 2.

3.2. Photoconductivity

Porphyrin nanostructures may demonstrate some degree of conductivity [19, 20, 22-27, 49-51] due to intermolecular transfer or delocalization of the excitation energy in their nanostructures, which generates photoconductance. Most studies so far have dealt with the J-aggregate nanorods self-assembled from metal-free porphyrins [23-28] as it was discussed in the introduction section. Frenkel exciton transport was also extensively studied and discussed in the tubular J-aggregates of the H_4TPPS^{2-} self-assembly [30, 52, 53]. Shelnutt et al. [6] observed photoconductance of metalloporphyrin binary nanostructures of $ZnTPPS^{4-}$ - SnT(N-EtOH-4-Py)P^{4+} and explained this by applying the charge-transfer exciton theory [6, 45]. This implies the existence of a configuration comprising the hole and the electron on different molecules, which are charge carriers at the applied potential. Systems were also reported in which the charge carriers exhibit both metal and ligand properties and were able to move between the metal and the macrocycle as well as between one molecule and its neighbor along a conducting metallomacrocycle stack [54].

These hypotheses may explain the existence of photoconductivity in the nanostructures of the H_4TPPS^{2-} - CoT(4-Py)P^{4+} system. Photoconductance measurements of the H_4TPPS^{2-} - CoT(4-Py)P^{4+} nanostructures were performed in the absence (dark current) and presence of illumination by visible light, Fig. 6. The nanostructures were applied to the surface of the electrode arrays (see experimental and Fig. S4 for details) by drop casting and subsequent washing and drying steps. Upon switching on the light, about a 10-fold increase in the current,

a photocurrent, at 0.5 V is observed compared to the dark current over the 400 nm distance between the contact electrodes (electrode gap), Fig. 5 A. The photoconductivity of the nanostructures was thus found to be $(5.1\pm1.3)\times10^{-5}$ S m^{-1} (n=5). We consider the photoconductivity thus found as the apparent photoconductivity, since the light excitation of the upper and the lower layers of the sample might be different.

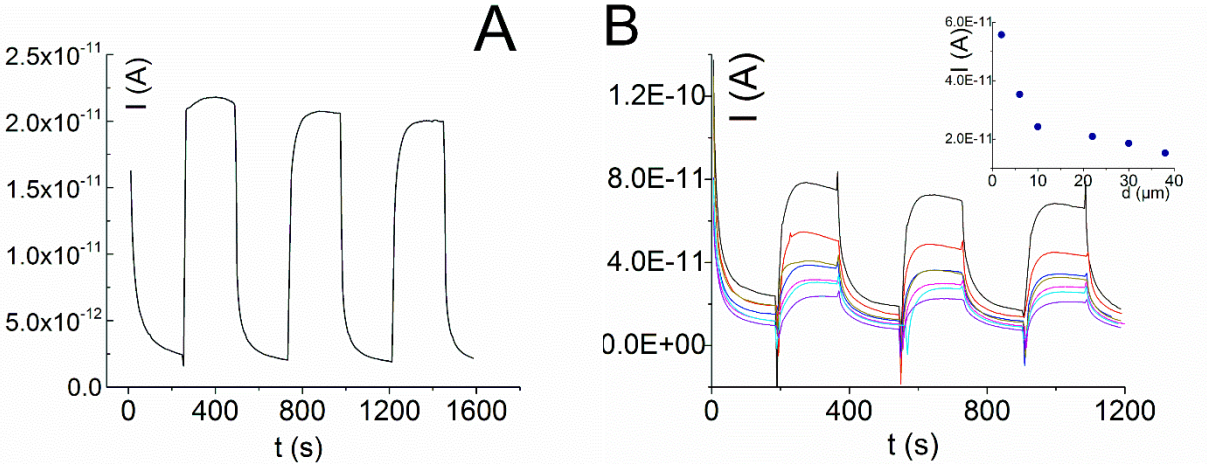

Figure 5. (A) Photocurrent of the H_4TPPS^{2-} - $CoT(4\text{-}Py)P^{4+}$ porphyrin nanostructures on the electrodes with a 400 nm gap. (B) dependence of the photocurrent of the H_4TPPS^{2-} - $CoT(4\text{-}Py)P^{4+}$ porphyrin nanostructures on the distance between interdigitated electrodes, V_{app}=0.5 V.

The dependence of the photocurrent on the path length, Fig. 5 B, was determined using an interdigitated electrode array and demonstrated a clear dependence between a photocurrent of the porphyrin nanostructures on the electrode distances with the photocurrent decreasing over the μm distances.

Table 1. (Photo)conductivity of porphyrin nanostructures.

Porphyrin NS	Conductivity, σ, S m^{-1}	Reference
P(V)-porphyrin-oligothiophene polymers[a]	1.2×10^{-7} - 5.1×10^{-6}	[55]
Tetraphenylporphine (TPP) film[b]	1.5×10^{-7}	[19]
TPP nanodots by self-assembly measured by the conductive-probe AFM[c]	0.046	[31]

Charge-transfer complexes of Lanthanide(III) bis(porphyrin) sandwiches and Zr(IV) bis(porphyrin) sandwiches[d]	8×10^{-3}	[49]
TPyP:TSPP crystalline rods[e]	9.3×10^{-8}	[27]
TMPyP:TSPP crystalline rods[f]	4.0×10^{-10}	[26]
Sn(IV)TPPS-Co(III)T(4-Py)P[g]	6×10^{-7}	[7]
H_4TPPS^{2-} - Co(III)T(4-Py)P^{4+} [g]	5×10^{-5}	this work

[a] conductivity value is given. The conductivity was enhanced by the photoirradiation. In the case of photoirradiation by 500 W Xe lamp through UV and IR cut-off filters, the enhancement was greater than threefold [55]; [b] crystalline films measured in vacuum; [c] the size of nanodots corresponded to ca. 5-7 layers of porphyrin. The conductivity along the vertical direction of the nanodots was measured; [d] conductivity; [e] 405 nm, 10 kW m^{-2}, 2 V bias; [f] 445 nm, 10 kW m^{-2}; [g] visible light, Xe lamp, 0.25 kW m^{-2}, 0.5 V bias.

The temperature dependence of the photoconductivity of the nanotubes displayed metal-like ($d\sigma/dT<0$) behavior of the changing current with increasing temperature, Fig. 6. This metal-like behavior is similar to the photoconductivity of Sn(IV)TPPS-Co(III)T(4-Py)P nanostructures [7] and might be due to electron-hole recombination or overcoming the energy of different types of intermolecular interactions and increased disorder with increasing temperature. Unfortunately, there is no consistent theoretical explanation for the conductance of similar systems, the temperature dependence, and, in particular, insufficient data are available on the carrier nature and properties for the (metallo)porphyrin nanostructures. Metallic behavior of the conductance ($d\sigma/dT<0$) was found in a TTF/TCNQ 1:1 donor-acceptor complex in a narrow temperature range [32], single-crystal $(SN)_x$ [56, 57], and stacked metallo-macrocycles (porphyrins and phthalocyanines) in the presence of an iodine acceptor [21, 54]. In our study, the presence of the iodine acceptor induced by treatment with I_2 vapor for 1.5 h resulted in an increase of the dark conductance as measured in a chemiresistor sensing mode [58], Fig. 6 B.

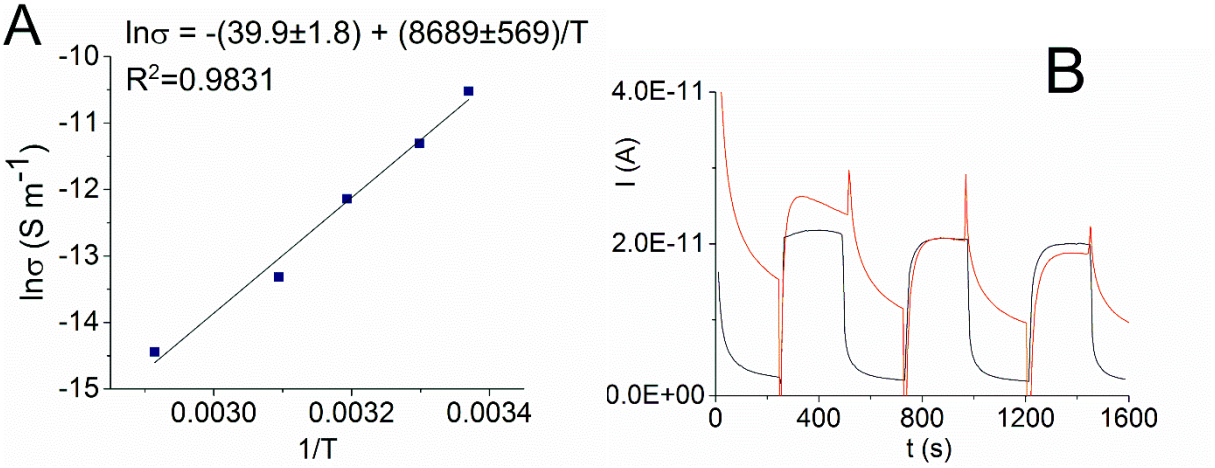

Figure 6. Dependence of the visible light apparent photoconductivity of the H_4TPPS^{2-} - $CoT(4\text{-}Py)P^{4+}$ nanostructures on A - temperature and B - I_2 treatment, Vapp=0.5V.

The apparent photoconductivity of this system is thus essentially higher than the apparent photoconductivity found previously for the Sn(IV)TPPS-Co(III)T(4-Py)P nanostructures of 6×10^{-7} S m^{-1} [7], Table 1, and is close to the photoconductivity of the H_4TPPS - Sn(IV)TPyP nanostructures, which have recently been prepared and are under study in our laboratory. The photoconductivity is comparable with the photoconductivity of the P^V porphyrin(electron acceptor)-oligothiophene(electron donor) polymer wires [55], Table 1. In the case of H_4TPPS^{2-} - $CoT(4\text{-}Py)P^{4+}$ (this work), H_4TPPS^{2-} - SnTPPyP, and Zn/Sn cloves (photoconductivity was not quantitatively estimated [6]), the nanostructures demonstrate J-aggregate absorbance bands near 490 nm and 706 nm, while SnTPPS-$CoT(4\text{-}Py)P^{4+}$ nanostructures do not exhibit these bands [7], which might be due to the longer intermolecular distances or weaker intermolecular interactions. This might explain the higher photoconductivities in the first two systems due to exciton delocalization [6, 30]. The data are in agreement with the generally low conductivity of the porphyrin molecules, which occupy an intermediate position between semiconductors and insulators [20]. Further fundamental investigations would be necessary to elucidate the details of the mechanism of photoconductivity in porphyrin nanostructures incorporating metalloporphyrin with a central metal such as Co(III), which readily participates in redox reactions.

Conclusion.

Molecular self-assembly of *meso*-tetrakis(4-sulfonatophenyl)porphine and Co(III) *meso*-tetra(4-pyridyl)porphine chloride has been shown to be an effective strategy for the easy preparation of binary porphyrin nanostructures exhibiting photoconductivity over μm distances.

A metal-like dependence of the photoconductance on temperature and dependence of the photocurrent of the porphyrin nanostructures on the μm electrode distances was demonstrated. The tunable characteristics of porphyrin nanoarchitectonics due to the great variability of their electronic and steric characteristics give raise to interest in investigating the self-assembled porphyrin nanostructures from the point of view of photo-induced energy and charge transfer as well as exciton engineering in materials according to structure.

Acknowledgements

The authors gratefully acknowledge Saint-Petersburg State University for a research grant 12.38.218.2015. We thank Dr. S. Willbold (Central Institute for Engineering, Electronics and Analytics - ZEA-3) for the NMR of porphyrin nanostructures, Dr. M. Heggen (Ernst Ruska-Centre) for the TEM investigations, E. Brauweiller-Reuters for the SEM investigations, Dr. I. Muratova, and V. Schöps for the thin film metal electrodes.

References

[1] D. Dolphin, Spectro-electrochemistry: porphyrins and metalloporphyrins, in: R.V. Bensasson, G. Jori, E.J. Land, T.G. Truscott (Eds.) Primary Photo-Processes in Biology and Medicine, Springer US, Boston, MA, 1985, pp. 171-180.
[2] S. Fukuzumi, H. Imahori, Biomimetic electron-transfer Chemistry of porphyrins and metalloporphyrins, in: V. Balzani (Ed.) Electron Transfer in Chemistry, Wiley-VCH Verlag GmbH 2008, pp. 927-975.
[3] T. Mirkovic, E.E. Ostroumov, J.M. Anna, R. van Grondelle, Govindjee, G.D. Scholes, Light absorption and energy transfer in the antenna complexes of photosynthetic organisms, Chemical Reviews, 117 (2017) 249-293.
[4] J.H. Fuhrhop, Porphyrin assemblies and their scaffolds, Langmuir, 30 (2014) 1-12.
[5] W. Auwarter, D. Ecija, F. Klappenberger, J.V. Barth, Porphyrins at interfaces, Nat Chem, 7 (2015) 105-120.
[6] K.E. Martin, Z. Wang, T. Busani, R.M. Garcia, Z. Chen, Y. Jiang, Y. Song, J.L. Jacobsen, T.T. Vu, N.E. Schore, B.S. Swartzentruber, C.J. Medforth, J.A. Shelnutt, Donor−acceptor biomorphs from the ionic self-assembly of porphyrins, Journal of the American Chemical Society, 132 (2010) 8194-8201.
[7] E.A. Koposova, A.A. Pendin, Y.E. Ermolenko, G.I. Shumilova, A.A. Starikova, Y.G. Mourzina, Morphological properties and photoconductivity of self-assembled Sn/Co porphyrin nanostructures, Rev. Adv. Mater. Sci., 45 (2016) 15-19.
[8] N. Micali, A. Romeo, R. Lauceri, R. Purrello, F. Mallamace, L.M. Scolaro, Fractal structures in homo- and heteroaggregated water soluble porphyrins, The Journal of Physical Chemistry B, 104 (2000) 9416-9420.
[9] D.M. Guldi, H. Imahori, Supramolecular assemblies for electron transfer, J. Porphyrins Phthalocyanines, 8 (2004) 976-983.
[10] C.M.R. Almeida, B.F.O. Nascimento, M. Pineiro, A.J.M. Valente, Thermodynamic study of the interaction between 5,10,15,20-tetrakis-(N-methyl-4-pyridyl)porphyrin tetraiodine and sodium dodecyl sulfate, Colloids and Surfaces A: Physicochemical and Engineering Aspects, 480 (2015) 279-286.

[11] R. Ge, X. Wang, C. Zhang, S.-Z. Kang, L. Qin, G. Li, X. Li, The influence of combination mode on the structure and properties of porphyrin–graphene oxide composites, Colloids and Surfaces A: Physicochemical and Engineering Aspects, 483 (2015) 45-52.
[12] X. Li, L. Zhang, J. Mu, Formation of new types of porphyrin H- and J-aggregates, Colloids and Surfaces A: Physicochemical and Engineering Aspects, 311 (2007) 187-190.
[13] H. Zhang, Y. Ma, Z. Lu, Z.-Z. Gu, Self-assembly films of tetrakis(hydroxyphenyl) porphyrins, Colloids and Surfaces A: Physicochemical and Engineering Aspects, 257-258 (2005) 291-294.
[14] U. Michelsen, C.A. Hunter, Self-assembled porphyrin polymers, Angewandte Chemie International Edition, 39 (2000) 764-767.
[15] D.-J. Qian, H.-T. Chen, B. Liu, X.-M. Xiang, T. Wakayama, C. Nakamura, J. Miyake, Monolayers and Langmuir-Blodgett films of palladium-mediated multiporphyrin arrays with different central ions, Colloids and Surfaces A: Physicochemical and Engineering Aspects, 284-285 (2006) 180-186.
[16] Y. Miyake, H. Tanaka, T. Ogawa, Scanning tunneling microscopy investigation of vanadyl and cobalt(II) octaethylporphyrin self-assembled monolayer arrays on graphite, Colloids and Surfaces A: Physicochemical and Engineering Aspects, 313-314 (2008) 230-233.
[17] Z. Wang, C.J. Medforth, J.A. Shelnutt, Porphyrin nanotubes by ionic self-assembly, Journal of the American Chemical Society, 126 (2004) 15954-15955.
[18] K.E. Martin, Y. Tian, T. Busani, C.J. Medforth, R. Franco, F. van Swol, J.A. Shelnutt, Charge effects on the structure and composition of porphyrin binary ionic solids: ZnTPPS/SnTMePyP nanomaterials, Chemistry of Materials, 25 (2013) 441-447.
[19] J.W. Weigl, Spectroscopic properties of organic photoconductors. Part IV. Tetraphenylporphine, Journal of molecular spectroscopy, 1 (1957) 216-222.
[20] N. Kobayashi, W. Andrew Nevin, S. Mizunuma, H. Awaji, M. Yamaguchi, Ring-expanded porphyrins as an approach towards highly conductive molecular semiconductors, Chemical Physics Letters, 205 (1993) 51-54.
[21] O.A. Golubchikov, B.D. Berezin, Applied aspects of the chemistry of porphyrins, Uspehi Chimii, 8 (1986) 1361-1389.
[22] A.A. Kocherzhenko, S. Patwardhan, F.C. Grozema, H.L. Anderson, L.D.A. Siebbeles, Mechanism of charge transport along zinc porphyrin-based molecular wires, Journal of the American Chemical Society, 131 (2009) 5522-5529.
[23] B.A. Friesen, B. Wiggins, J.L. McHale, U. Mazur, K.W. Hipps, Differing HOMO and LUMO mediated conduction in a porphyrin nanorod, Journal of the American Chemical Society, 132 (2010) 8554-8556.
[24] A.L. Yeats, A.D. Schwab, B. Massare, D.E. Johnston, A.T. Johnson, J.C. de Paula, W.F. Smith, Photoconductivity of self-assembled nanotapes made from *meso*-tri(4-sulfonatophenyl)monophenylporphine, The Journal of Physical Chemistry C, 112 (2008) 2170-2176.
[25] A.D. Schwab, D.E. Smith, B. Bond-Watts, D.E. Johnston, J. Hone, A.T. Johnson, J.C. de Paula, W.F. Smith, Photoconductivity of self-assembled porphyrin nanorods, Nano Letters, 4 (2004) 1261-1265.
[26] M. Adinehnia, B. Borders, M. Ruf, B. Chilukuri, K.W. Hipps, U. Mazur, Comprehensive structure–function correlation of photoactive ionic π-conjugated supermolecular assemblies: an experimental and computational study, Journal of Materials Chemistry C, 4 (2016) 10223-10239.
[27] B. Borders, M. Adinehnia, N. Rosenkrantz, M. van Zijll, K.W. Hipps, U. Mazur, Photoconductive behavior of binary porphyrin crystalline assemblies, J. Porphyrins Phthalocyanines, 21 (2017) 569-580.
[28] C.K. Riley, E.A. Muller, B.E. Feldman, C.M. Cross, K.L.V. Aken, D.E. Johnston, Y. Lu, A.T. Johnson, J.C.d. Paula, W.F. Smith, Effects of O2, Xe, and gating on the photoconductivity

and persistent photoconductivity of porphyrin nanorods, The Journal of Physical Chemistry C, 114 (2010) 19227-19233.
[29] M. Vasilopoulou, D.G. Georgiadou, A.M. Douvas, A. Soultati, V. Constantoudis, D. Davazoglou, S. Gardelis, L.C. Palilis, M. Fakis, S. Kennou, T. Lazarides, A.G. Coutsolelos, P. Argitis, Porphyrin oriented self-assembled nanostructures for efficient exciton dissociation in high-performing organic photovoltaics, Journal of Materials Chemistry A, 2 (2014) 182-192.
[30] T. Zhu, Y. Wan, L. Huang, Direct imaging of Frenkel exciton transport by ultrafast microscopy, Accounts of Chemical Research, 50 (2017) 1725–1733.
[31] X. Zhai, N.M.K.K. Arachchige, P. Derosa, J.C. Garno, Conductive-probe measurements with nanodots of free-base and metallated porphyrins, Journal of Colloid and Interface Science, 486 (2017) 38-45.
[32] J. Ferraris, V. Walatka, J. Perlstein, D.O. Cowan, Electron-transfer in a new highly conducting donor-acceptor complex, Journal of the American Chemical Society, 95 (1973) 948-949.
[33] M. Natali, F. Scandola, Photoinduced charge separation in porphyrin ion pairs, The Journal of Physical Chemistry A, 120 (2016) 1588-1600.
[34] M.-S. Choi, T. Yamazaki, I. Yamazaki, T. Aida, Bioinspired molecular design of light-harvesting multiporphyrin arrays, Angewandte Chemie International Edition, 43 (2004) 150-158.
[35] J.-H. Ha, H.S. Cho, J.K. Song, D. Kim, N. Aratani, A. Osuka, Excitonic coupling strength and coherence length in the singlet and triplet excited states of meso–meso directly linked Zn(II)porphyrin arrays, ChemPhysChem, 5 (2004) 57-67.
[36] M.E. El-Khouly, S. Fukuzumi, F. D'Souza, Photosynthetic antenna–reaction center mimicry by using boron dipyrromethene sensitizers, ChemPhysChem, 15 (2014) 30-47.
[37] H. Tajima, K. Shimatani, T. Komino, S. Ikeda, M. Matsuda, Y. Ando, H. Akiyama, Light-emitting diodes fabricated from biomolecular compounds, Colloids and Surfaces A: Physicochemical and Engineering Aspects, 284-285 (2006) 61-65.
[38] T. Akiyama, A. Miyazaki, M. Sutoh, I. Ichinose, T. Kunitake, S. Yamada, Fabrication of porphyrin–titanium oxide–fullerene assemblies on an ITO electrode and their photocurrent responses, Colloids and Surfaces A: Physicochemical and Engineering Aspects, 169 (2000) 137-141.
[39] F. Dini, E. Martinelly, G. Pomarico, R. Paolesse, D. Monti, D. Filippini, A. D'Amico, I. Lundström, C. Di Natale, Chemical sensitivity of self-assembled porphyrin nano-aggregates., Nanotechnology, 20 (2009) 055502.
[40] B. Sandrino, C.d.S. Clemente, T.M.B.F. Oliveira, F.W.P. Ribeiro, F.J. Pavinatto, S.E. Mazzetto, P. de Lima-Neto, A.N. Correia, C.A. Pessoa, K. Wohnrath, Amphiphilic porphyrin-cardanol derivatives in Langmuir and Langmuir–Blodgett films applied for sensing, Colloids and Surfaces A: Physicochemical and Engineering Aspects, 425 (2013) 68-75.
[41] S. Sengupta, F. Würthner, Chlorophyll J-aggregates: from bioinspired dye stacks to nanotubes, liquid crystals, and biosupramolecular electronics, Accounts of Chemical Research, 46 (2013) 2498-2512.
[42] R.E. Andernach, S. Rossbauer, R.S. Ashraf, H. Faber, T.D. Anthopoulos, I. McCulloch, M. Heeney, H.A. Bronstein, Conjugated polymer–porphyrin complexes for organic electronics, ChemPhysChem, 16 (2015) 1223-1230.
[43] A.K. Burrell, M.R. Wasielewski, Porphyrin-based nanostructures: routes to molecular electronics, J. Porphyrins Phthalocyanines, 04 (2000) 401-406.
[44] R. Lauceri, S. Gurrieri, E. Bellacchio, A. Contino, L. Monsu'scolaro, A. Romeo, A. Toscano, R. Purrello, J-type aggregates of the anionic meso-tetrakis(4-sulfonatophenyl)porphine induced by ‚hindered' cationic porphyrins, Supramolecular Chemistry, 12 (2000) 193-202.

[45] E.V.M. Agranovich, G.F. Bassani, Electronic excitations in organic based nanostructures, Elsevier Academic Press2003.
[46] O. Ohno, Y. Kaizu, H. Kobayashi, J-aggregate formation of a water-soluble porphyrin in acidic aqueous media, The Journal of Chemical Physics, 99 (1993) 4128-4139.
[47] M.M. Kruk, S.E. Braslavsky, Acid−base equilibria in 5,10,15,20-tetrakis(4-sulfonatophenyl)chlorin: role of conformational flexibility, The Journal of Physical Chemistry A, 110 (2006) 3414-3425.
[48] E.B. Fleischer, L.E. Webb, The Basicity in Water of α,β,γ,δ-tetra-(4-pyridyl)-porphine, The Journal of Physical Chemistry, 67 (1963) 1131-1133.
[49] J.P. Collman, J.L. Kendall, J.L. Chen, K.A. Collins, J.-C. Marchon, Formation of charge-transfer complexes from neutral bis(porphyrin) sandwiches, Inorganic Chemistry, 39 (2000) 1661-1667.
[50] C.M. Drain, Self-organization of self-assembled photonic materials into functional devices: Photo-switched conductors PNAS, 99 (2002) 5178-5182.
[51] S.M. Kuzmin, S.A. Chulovskaya, M.V. Tesakova, A.S. Semeikin, V.I. Parfenyuk, Solvent and electrode influence on electrochemical forming of poly-Fe(III)-aminophenylporphyrin films, J. Porphyrins Phthalocyanines, 21 (2017) 555-567.
[52] A. Huijser, T.J. Savenije, J.E. Kroeze, L.D.A. Siebbeles, Exciton diffusion and interfacial charge separation in meso-tetraphenylporphyrin/TiO_2 bilayers: effect of ethyl substituents, The Journal of Physical Chemistry B, 109 (2005) 20166-20173.
[53] S.M. Vlaming, R. Augulis, M.C.A. Stuart, J. Knoester, P.H.M. van Loosdrecht, Exciton spectra and the microscopic structure of self-assembled porphyrin nanotubes, The Journal of Physical Chemistry B, 113 (2009) 2273-2283.
[54] B.M. Hoffman, J.A. Ibers, Porphyrinic molecular metals, Acc. Chem. Res., 16 (1983) 15-21.
[55] H. Segawa, N. Nakayama, T. Shimidzu, Electrochemical synthesis of one-dimensional donor–acceptor polymers containing oligothiophenes and phosphorus porphyrins, J. Chem. Soc., Chem. Commun., (1992) 784-786.
[56] V.V.J. Walatka, M.M. Labes, J.H. Perlstein, Polysulfur nitride - a one-dimensional chain with a metallic ground state, Physical Review Letters, 31 (1973) 1139-1142.
[57] L. Pintschovius, Polysulfur nitride, (SN)x , the first example of a polymeric metal, Colloid & Polymer Sci., 256 (1978) 883-892.
[58] I.S. Muratova, K.N. Mikhelson, Y. Ermolenko, A. Offenhäusser, Y. Mourzina, On “resistance overpotential” caused by a potential drop along the ultrathin high aspect ratio gold nanowire electrodes in cyclic voltammetry, Journal of Solid State Electrochemistry, 20 (2016) 3359-3365.